AIAA 2003-1813

Active/Passive Control of Sound Radiation from Panels using Constrained Layer Damping

Gary P. Gibbs, Randolph H. Cabell
NASA Langley Research Center, Hampton, VA 23681

11th AIAA/ASME/AHS Adaptive Structures Conference
April 7–10, 2003/Norfolk, VA

For permission to copy or republish, contact the American Institute of Aeronautics and Astronautics 1801 Alexander Bell Drive, Suite 500, Reston, VA 20191–4344

ACTIVE/PASSIVE CONTROL OF SOUND RADIATION FROM PANELS USING CONSTRAINED LAYER DAMPING

Gary P. Gibbs*, Randolph H. Cabell†
NASA Langley Research Center, Hampton, VA 23681

A hybrid passive/active noise control system utilizing constrained layer damping and model predictive feedback control is presented. This system is used to control the sound radiation of panels due to broadband disturbances. To facilitate the hybrid system design, a methodology for placement of constrained layer damping which targets selected modes based on their relative radiated sound power is developed. The placement methodology is utilized to determine two constrained layer damping configurations for experimental evaluation of a hybrid system. The first configuration targets the (4,1) panel mode which is not controllable by the piezoelectric control actuator, and the (2,3) and (5,2) panel modes. The second configuration targets the (1,1) and (3,1) modes. The experimental results demonstrate the improved reduction of radiated sound power using the hybrid passive/active control system as compared to the active control system alone.

Introduction

There has been considerable interest over the past several years in applying feedback control methods to problems of structural acoustics. The structural acoustics problem typically requires a control bandwidth that extends to several hundred Hertz, and thus a digital controller would have to operate at a few kiloHertz.

To be practical, structural acoustic control requires a simple plant model that can be updated quickly with reasonable computational requirements. Recent papers by the authors[1,2] discussed one way to simplify a feedback controller, by reducing the number of actuators and sensors needed for good performance. The work was done on a tensioned aircraft-style panel excited on one side by turbulent boundary layer (TBL) flow in a low speed wind tunnel. Actuation was provided by a lead zirconium titanate (PZT) piezoceramic actuator mounted on the center of the panel. For sensing, the responses of four accelerometers, positioned to sense an approximate response of the first radiation mode of the panel, were summed and fed back through the controller. This single input-single output topology was found to have nearly the same noise reduction performance as a controller with fifteen accelerometers and three PZT patches.[1,2]

This paper extends the previous results by looking at how constrained layer damping (CLD) on a panel can be used to enhance the performance of the feedback controller thus providing a more robust and efficient hybrid active/passive system. The eventual goal is to use the CLD to reduce vibration at selected modes to enhance performance and robustness, and then implement a simple, reduced order, low sample rate adaptive controller to attenuate sound radiation at low frequencies. Additionally the added damping provided by the CLD smoothes phase transitions over the bandwidth which promotes robustness to resonant frequency shifts. A methodology is also presented which permits the placement of CLD patches in locations which target selected modes based on their sound radiation. The relative weighting of each mode in the placement cost function is based on sound radiation of that mode and not necessarily vibrational energy. This work is an extension of the work previously presented by the authors.[3]

Experiments were conducted in the NASA Langley Research Center Transmission Loss Apparatus on a clamped-clamped aluminum panel driven on one side by a loudspeaker. A generalized predictive control (GPC) algorithm, which is suited to online adaptation of its parameters,[4] was used in single input-single output (SISO) and multiple input-single output (MIMO) configurations. Because this was a preliminary look at the potential of constrained layer damping for adaptive control, static feedback control was used. Two configurations of CLD in addition to a bare panel configuration were studied. For each CLD configuration, two sensor arrangements for the feedback controller were compared. The first arrangement used fifteen accelerometers on the panel to estimate the responses of the first six radiation modes of the panel.[5] The second sensor arrangement was simpler, using the summed responses of only four accelerometers to approximate the response of the first radiation mode of the panel.[1,2] In all cases a PZT patch was mounted at the center of the panel for control input. The performance of the controller was quantified using the responses of the fifteen accelerometers on the panel to estimate radiated sound power.

Constrained Layer Damping Placement

Constrained layer damping provides energy dissipation through dynamic shear strains of a viscoelastic material. This material is subjected to shear between

*Structural Acoustics Branch, Member AIAA
†Structural Acoustics Branch

the base structure and the CLD face sheet. The CLD is most effective in regions of the structure that undergo maximum curvature. Thus particular modes can be selectively damped by placement of CLD in regions of maximum curvature for that mode.

In this section the methodology for constrained layer damping placement will be presented. It is important that the active and passive treatments work in concert to reduce the overall radiated sound. For this paper, the CLD was designed to provide a combination of reduction of the high frequency odd-odd panel modes (efficient radiators), and modes uncontrollable by the PZT.

Following the work by Plunkett and Lee,[6] if we consider a 1-D beam covered with a segment of length l of constrained layer damping the energy loss per cycle can be expressed as:

$$L_B = C_B \int_l \left(\frac{d^2z}{dx^2}\right)^2 dx \tag{1}$$

where L_B is the energy loss per cycle ($Nm/cycle$), C_B is a constant including the modulus of elasticity and thickness, z is the out of plane displacement, x is the coordinate along the beam axis, and the term $\frac{d^2z}{dx^2}$ is the curvature of the beam. Thus the dissipation is proportional to the integral of the curvature squared under the CLD patch. This concept can be generalized to a two dimensional plate as:

$$L_P = C_P \int_S \left(\nabla^2 z\right)^2 dS \tag{2}$$

where L_P is the energy loss per cycle for the plate, C_P is a constant including the modulus of elasticity and plate thickness, and $\nabla^2 z$ is the curvature of the plate in x and y directions, and S is the surface area of the CLD. Thus if the surface area of the CLD, S, corresponds to the surface area of the plate, S_P, then the loss will be a maximum for a given type of CLD:

$$L_{Pmax} = C_P \int_{S_P} \left(\nabla^2 z\right)^2 dS. \tag{3}$$

If S corresponds to a sub-area of the plate that has relatively low curvature then the loss will be much less than the maximum. If the sub-area includes high curvature regions then the loss could be almost as high as the maximum. The percentage of possible absorption by a CLD patch over a sub-area, S, is:

$$\%L = 100\frac{L_P}{L_{Pmax}} \tag{4}$$

The $\%L$ of equation 4 is termed the effective absorption percentage. The loss factor for each mode can be examined independently. Thus for the m-th mode the energy loss per cycle is:

$$L_{P_m} = C_P \int_S \left(\nabla^2 z_m\right)^2 dS \tag{5}$$

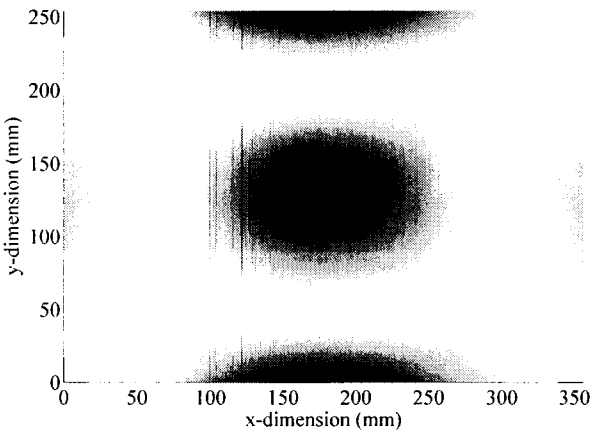

Figure 1 Curvature squared for mode (1,1)

where L_{p_m} is the energy loss per cycle for the m-th plate mode, and $\nabla^2 z_m$ is the curvature of the m-th mode. If S corresponds to the surface area of the plate, S_P, then the loss for the m-th mode will a maximum for a given type of CLD:

$$L_{Pmax_m} = C_P \int_{S_P} \left(\nabla^2 z_m\right)^2 dS \tag{6}$$

If the CLD covers regions of the plate that have highest curvature for mode m then the integrated loss will include most of the energy that would be absorbed with total coverage for mode m. Thus the percentage of possible absorption by a CLD patch over a sub-area, S for the m-th mode is:

$$\%L_m = 100\frac{L_{P_m}}{L_{Pmax_m}} \tag{7}$$

where the $\%L_m$ of equation 7 is termed the effective modal absorption percentage.

These concepts will be illustrated with an example on a $356mm \times 254mm \times 1mm$ clamped-clamped panel. Formulations for the natural frequencies and mode shapes of clamped-clamped plates can be found in Blevins,[7] and can be used to determine the curvature of selected modes. A plot of the curvature squared of the 1st mode of the clamped plate is shown in Figure 1 where black corresponds to the maximum curvature squared of the mode and white corresponds to zero curvature squared. The black outlined rectangle should be ignored for this discussion and will be addressed later. The curvature squared is large near the center and very close to the edges; therefore, a CLD patch placed at the center and covering most of the central region of the plate could absorb almost as much energy as a patch covering the entire plate for the first mode. Effective modal absorption percentage for various center-mounted CLD patches for mode 1 are presented in Table 1. Column 1 denotes the patch dimension (lx, ly). Column 2 denotes the corresponding

Table 1 Relative performance of CLD for Mode 1

Patch Dimension (mm)	% of total area	Effective Modal Absorption Pct.
112×80	10	36.9
178×127	25	56.4
251×180	50	61.1
356×254	100	100

Table 2 Performance of $50.8mm \times 101.6mm$ patch of CLD for various panel modes

Mode (m,n)	Effective Modal Absorption Pct.
(1,1)	23.6
(3,1)	15.5
(1,3)	19.3
(3,2)	2.69
(2,3)	5.07
(3,3)	9.76
(4,1)	15.3
(4,2)	2.56
(5,1)	11.0
(5,2)	1.72

area as a percentage of the total plate area. Column 3 is the effective modal absorption percentage, $\%L_m$. Note that with only 25% coverage of the plate the effective modal absorption percentage is 56%.

The effective modal absorption percentage was calculated for a $50.8mm \times 101.6mm$ CLD patch mounted in the center of the aforementioned panel. The results were examined for each mode and are summarized in Table 2. It can be seen that the results for each mode vary, the odd-odd modes tend to show a higher effective modal absorption percentage (and thus absorption), than the modes with even first and/or second indices. This methodology will permit the tailoring of the CLD treatment to selected modes and can work in concert with the active control system. Plots of the curvature squared over the panel are shown in Figures 1 through 10 for the modes presented in Table 2. The black outlined rectangle corresponds to the area covered by the CLD. Careful examination of Figures 1 through 10 with respect to the coverage of the CLD patch should clarify the results shown previously in Table 2.

For this paper the desired cost function is the reduction of radiated sound power. It is thus important to configure constrained layer damping treatments to target selected modes in terms of reducing their sound radiation, and not necessarily their ability to absorb vibrational energy. For example well below the acoustic coincidence frequency the (2,2) panel mode will typically radiate much less acoustic energy than the (1,1) mode and thus should receive much less emphasis in the placement procedure. To implement this procedure, panel modes were normalized to produced equal effective modal absorption percentage, $\%L_{Pmax_m}$, as shown previously in equation 6. Next measured data was obtained for the total radiated sound power of the panel for the given excitation (as discussed in the next section) to determine the relative modal contribution. Radiated sound power at or near the resonance of each mode was summed and stored. A relative radiation factor was determined for each mode by dividing the total radiated sound power of the m-th mode, R_m, by the total radiated sound power, R:

$$k_m = \frac{R_m}{R} \tag{8}$$

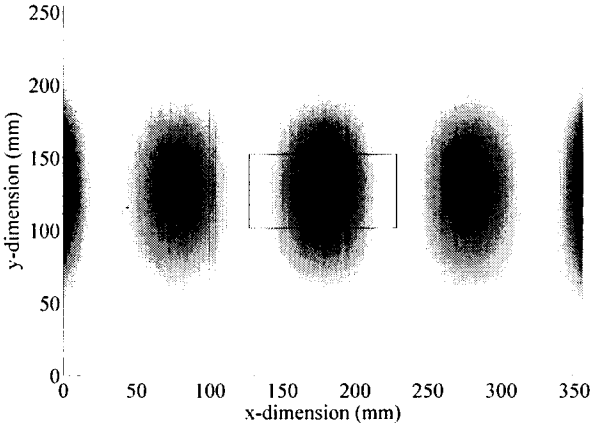

Figure 2 Curvature squared for mode (3,1)

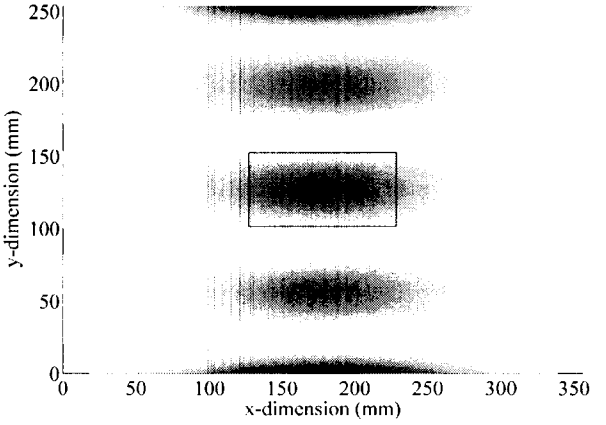

Figure 3 Curvature squared for mode (1,3)

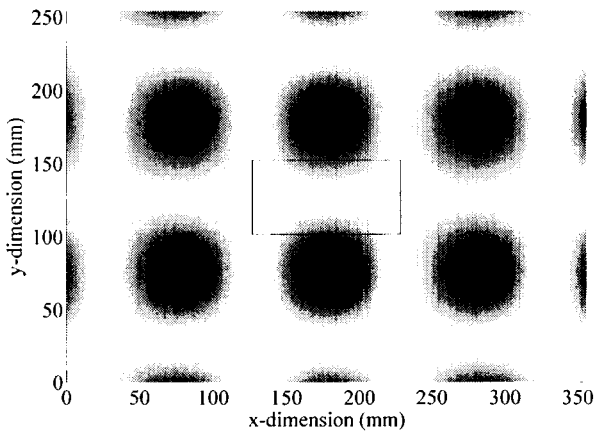

Figure 4 Curvature squared for mode (3,2)

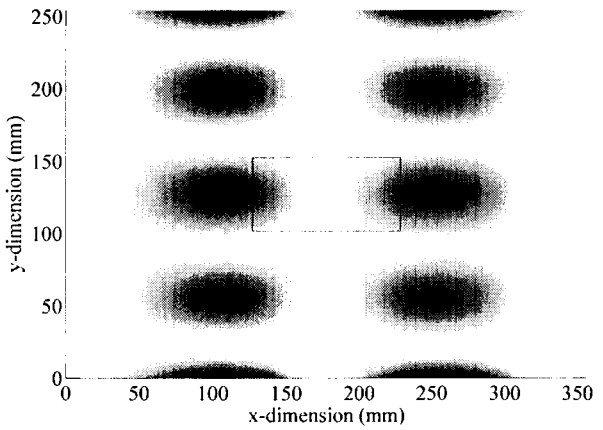

Figure 5 Curvature squared for mode (2,3)

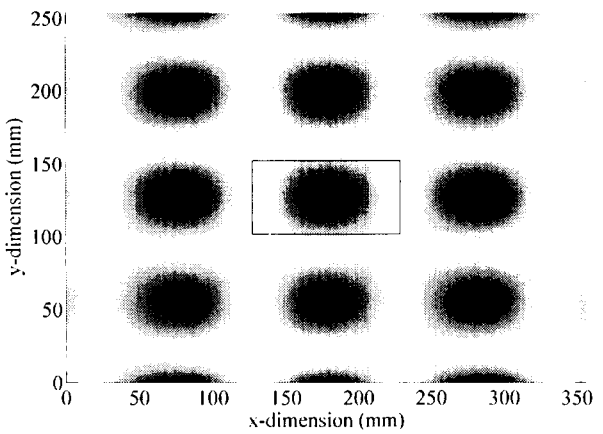

Figure 6 Curvature squared for mode (3,3)

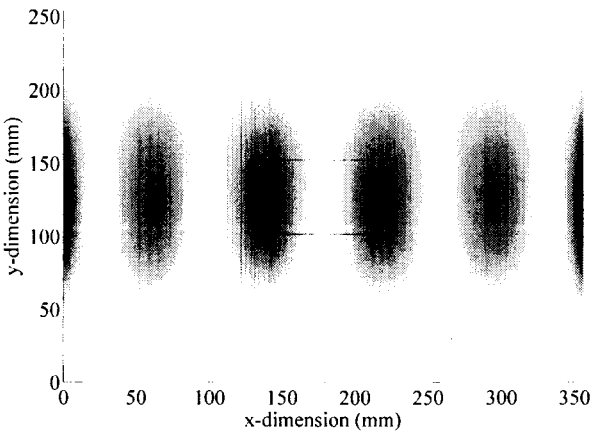

Figure 7 Curvature squared for mode (4,1)

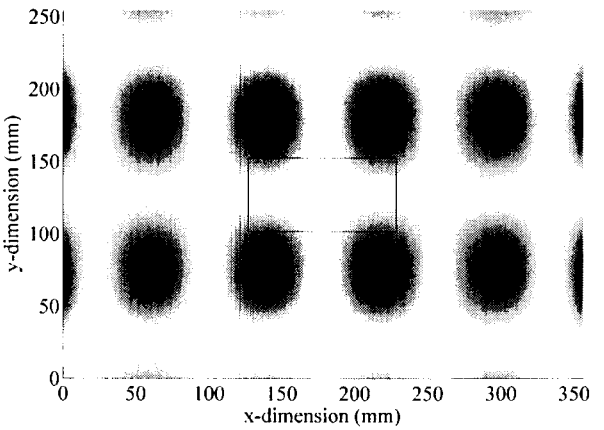

Figure 8 Curvature squared for mode (4,2)

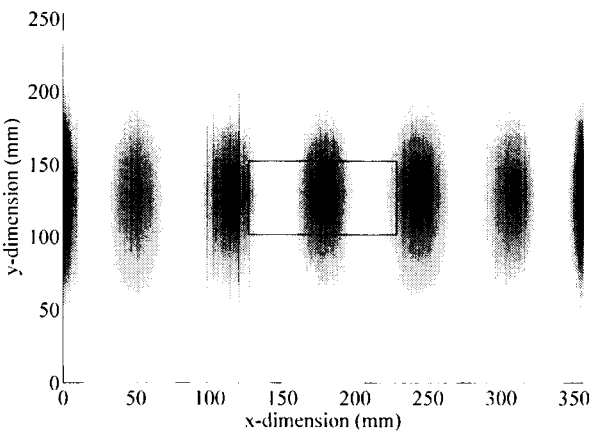

Figure 9 Curvature squared for mode (5,1)

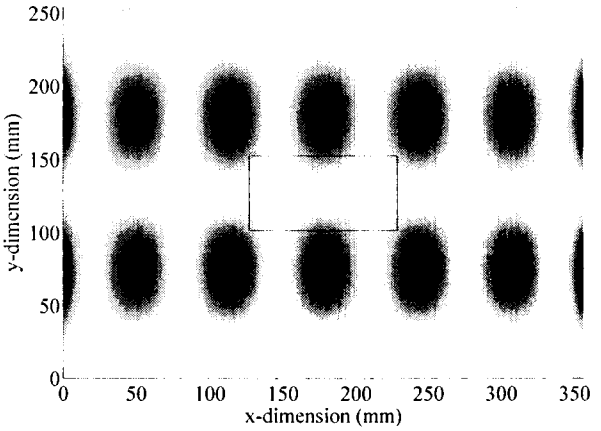

Figure 10 Curvature squared for mode (5,2)

where, k_m is the relative radiation factor.

The performance of candidate CLD locations was then evaluated using the following cost function:

$$J = \sum_{i=m}^{M} k_m L_{P_m} \tag{9}$$

where J is the cost value, and M is the total number of modes to be included. If modes are to be excluded from the analysis then those modes should be omitted from equation 9.

Two configurations of constrained layer damping, henceforth referred to as the A and B configurations, were tested in this study, and the performance results will be presented in the next section. For both configurations, one strip of $50.8mm \times 101.6mm$ CLD was placed on top of the PZT (corresponding to the black square in Figures 1 through 10) which is a high strain location for the odd-odd panel modes. The other two $50.8mm \times 101.6mm$ strips were placed in either the A or B locations in Figure 11. These locations were optimized with consideration of the curvature of panel modes that contributed significantly to sound radiation. The A locations were chosen so as to add damping to the (4,1) panel mode, which was not controllable by the PZT, and the (2,3) and (5,2) panel modes. The B locations were chosen to add damping to the (1,1) and (3,1) modes, in addition to the damping provided by the center strip of CLD.

Test Configuration

Testing was done on a $254mm \times 356mm \times 1mm$ thick aluminum panel clamped on all sides and mounted in a transmission loss facility. The panel is shown in the schematic in Figure 11. The dynamics of this panel are simpler than an actual aircraft panel, and the damping is also lower, but the structure was still useful for studying the influence of constrained layer damping on a feedback controller. A disturbance excitation was produced by a loudspeaker in the source room driven

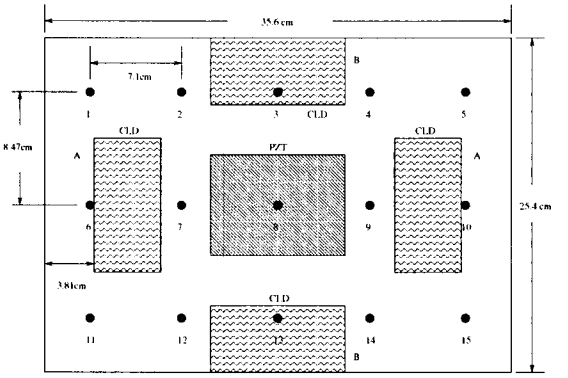

Figure 11 Accelerometers, PZT and CLD on Panel

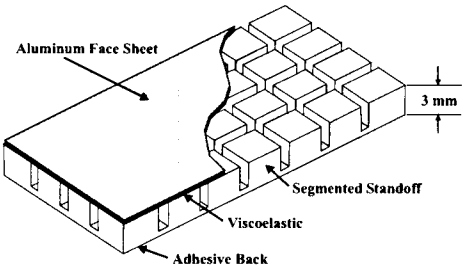

Figure 12 CLD configuration

with an 1000 Hz bandwidth random signal providing broadband excitation of the panel. Control actuation was provided with two PZT actuators, each measuring $110mm \times 38mm \times 0.76mm$ resulting in an effective $110mm \times 76mm \times 0.76mm$ actuator, mounted on the center of the source room side of the panel as illustrated in Figure 11. The actuator inputs were wired together, and so they appeared to the control system as a single actuator. Fifteen accelerometers, denoted by the numbered circles in Fig. 11, were mounted on the receiver room side of the panel. All fifteen accelerometers were used for the radiation mode controller, and accelerometers 3, 7, 9, and 13 were used for the simpler four-accelerometer controller.[1,2] Note that summing the time domain responses of these four accelerometers filters out the contributions of low order even modes, which are inefficient radiators of sound below the coincidence frequency.

The CLD material was $3mm$ thick, weighed $2.07kg/m^2$, and had regularly spaced grooves cut into the viscoelastic material as shown in Figure 12. Each configuration consisted of three strips of CLD, with dimensions $50.8mm \times 101.6mm$, on the source room side of the panel. The strips weighed a total of 30.2 g, or 12.6% of the mass of the bare panel, and covered 17.1% of the total panel area.

Control and data acquisition were handled by a PC-based system using TMS320C40 digital signal processors (DSP). The controller operated with a 2000 Hz

Table 3 Modal damping percentages

Mode	Damping (%)		
(horiz., vert.)	bare panel	A	B
(1,1)	1.6	2.7	4.3
(3,1)	0.8	6.4	4.1
(1,3)	1.1	5.4	4.6

sampling frequency and anti-aliasing and reconstruction filters set to 800 Hz. Controller performance was monitored using the 15 accelerometers sampled with a separate data acquisition system running at 5000 Hz sampling frequency.

Results

The passive damping results will be presented first followed by the active control results. In all cases, the controller performance is quantified in terms of reductions in radiated sound power using the elemental radiator approach[8] derived from the responses of the 15 accelerometers on the panel.

The passive damping provided by the CLD is summarized in terms of modal damping percentages in Table 3 and radiated sound power in Figure 13. The percentages in Table 3 indicate that both CLD configurations added significant damping to the odd-odd panel modes. In terms of radiated sound power shown in Figure 13 integrated from 50 to 800 Hz, the reduction was 7.1 dB for CLD at the A locations and 6.6 dB for CLD in the B locations. Both CLD configurations had a similar effect on the (1,1) mode: Integrated from 70 to 125 Hz, the radiated sound power was reduced by 5.2 dB and 5.7 dB for A and B respectively. From 400 to 600 Hz, which contains the natural frequencies of the (4,1) and (1,3) modes, the integrated reduction for A was 7.5 dB and for B was 7.0 dB. In spite of the similar reductions, the damping provided by the CLD between 400 and 600 Hz was very location dependent, with the A configuration adding significantly more damping to the (4,1) mode just above 400 Hz as desired.

Closed loop results for controlling responses of the first six radiation modes of the panel are shown in Fig. 14. The closed loop reduction in radiated sound power integrated from 50 to 800 Hz was 5.3 dB for the bare panel, 9.2 dB for the A CLD configuration, and 7.7 dB for B. Relative to the passively damped configurations with CLD only, the feedback controller produced additional reductions over the entire bandwidth of 2.1 dB for A and 1.1 dB for B. Although not readily visible in the figure, the (4,1) mode at 420 Hz and the (5,2) mode near 750 Hz were not controllable, so the bare panel results overlay the open loop results at those frequencies. Between 70 and 125 Hz, the B configuration performed slightly better than A, with a reduction of 8.9 dB to A's 7.8 dB. From 400 to 600 Hz,

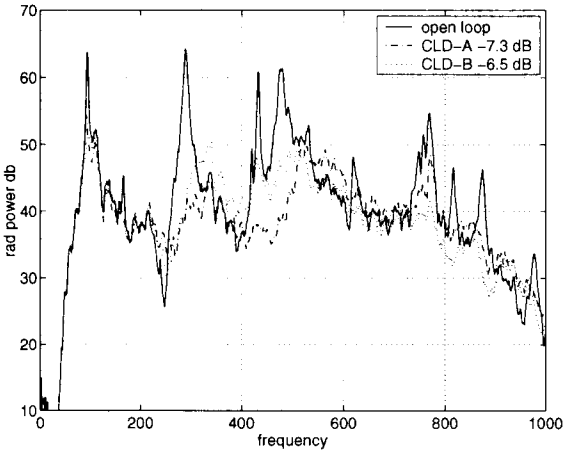

Figure 13 Performance of CLD

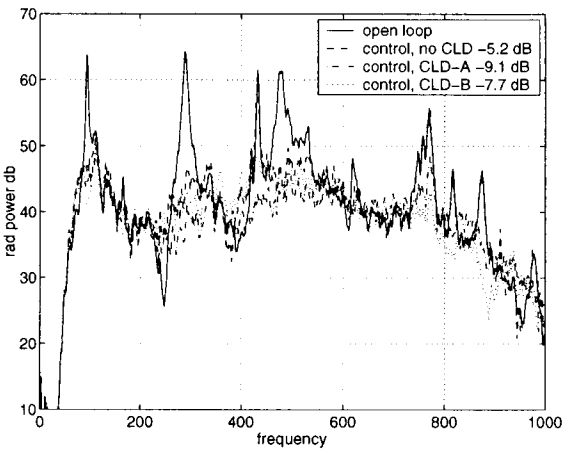

Figure 14 Radiation Mode Control

the A configuration reduced the radiated sound power by 10.1 dB, whereas the B configuration reduced it by only 7.5 dB. The difference appears to be due to reductions obtained at the (4,1) mode near 420 Hz.

The closed loop results for the simpler control configuration using only four accelerometers are shown in Figure 15. The bare panel results are not nearly as good as the bare panel results for the radiation mode controller. However, the reductions obtained with CLD in either configuration are relatively close to those obtained with the radiation mode controller. Integrated from 50 to 800 Hz, the reductions obtained were 3.0 dB for no CLD, 8.8 dB for the A CLD configuration, and 7.0 dB for the B configuration. Although not shown here, the controller in the bare panel case produced significant reductions in the controller cost function, which was the sum of the responses of the four accelerometers. This performance did not translate into significant reductions in radiated sound power. However, with CLD on the panel, reductions in the summed accelerometer responses did produce

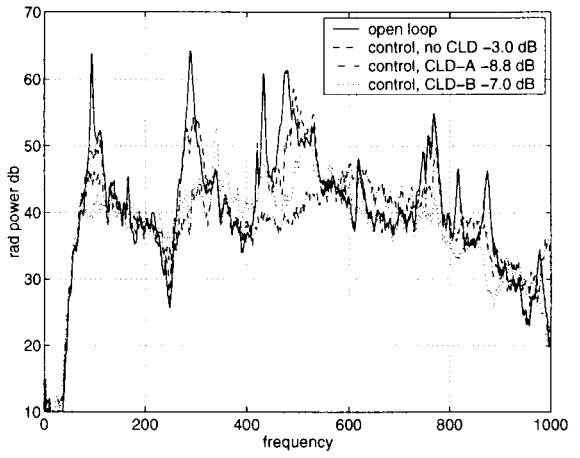

Figure 15 Diamond accelerometer pattern control

reductions in radiated sound power. A likely reason for this behavior is that the feedback controller was less aggressive when CLD was on the panel due to the significant amount of passive damping provided by the CLD. Because the controller was less aggressive, it was less likely to drive the panel in such a way as to increase radiated sound power in uncontrolled modes.

The simple controller was able to surpass the performance of the more complicated radiation mode controller in certain areas of the spectrum. The reduction integrated from 70 to 125 Hz was 9.7 dB and 13.1 dB for the A and B cases, respectively, both of which are greater than the reductions obtained with the radiation mode controller over that same bandwidth. From 400 to 600 Hz, the integrated reduction was 10.8 dB for the A configuration and 6.3 dB for the B configuration, which are, respectively, 0.7 dB more and 1.2 dB less than the radiation mode controller. The good performance of the simple controller was possible because the sound radiation from this panel in this frequency range was dominated by the first radiation mode of the structure. When the simple four accelerometer cost function provided a good approximation to the response of the first radiation mode, the simple controller performed well. This was most apparent for the A CLD configuration, because the simple cost function for this configuration closely matched the response of the first radiation mode near the (1,1) and (1,3) panel modes. The match was not as close for the B configuration, which could have been a result of a slight change in the boundary conditions due to the B CLD locations.

The closed loop performance of the simple controller with the A configuration is a promising start for simplifying the feedback controller with CLD. However, the sensitivity of performance to CLD location indicates that optimization of the CLD placement together with the controller cost function is a difficult problem that is tightly coupled with the disturbance spectrum and panel dynamics in the bandwidth of interest.

Summary

A CLD placement methodology based on sound radiation was presented. This placement methodology provided an effective means of determining optimum CLD locations for selected modes and was experimentally confirmed.

The hybrid active/passive control results described here illustrate how constrained layer damping (CLD) can help a simple feedback controller topology produce reductions in radiated sound power that are close to those of a much more complicated controller topology. The radiated sound power controller that required fifteen accelerometers whose outputs were processed to compute radiation mode responses, reduced the sound power by 9.2 dB. The results also illustrate that the impact of the CLD on the closed loop performance depends on the CLD's placement on the structure and on the control cost function. The simple controller was able to reduced the radiated sound power by over 8 dB which approaches that obtained by the radiation mode controller.

The results demonstrate that for this very simple system there is considerable benefit to designing the passive and active characteristics of the controller together. Careful optimization of the CLD placement and controller cost function can be used to implement a low bandwidth, reduced order feedback controller which would be amenable to online adaptation of the controller parameters. Considerable work remains to be done in order to apply this approach to the much more complicated dynamics of a real aircraft panel subject to varying flight conditions.

References

[1]Gibbs, G., Cabell, R., and Juang, J., "Controller Complexity for Active Control of TBL Induced Sound Radiation from Panels," *6th AIAA/CEAS Aeroacoustics Conference*, No. AIAA 2000-2043, Lahaina, Hawaii, June 12-14 2000.

[2]Gibbs, G. P., Cabell, R. H., and Juang, J., "Controller Complexity for Active Noise Control of Turbulent Boundary Layer Noise from Panels," *to appear AIAA Journal*, 2003.

[3]Cabell, R. H. and Gibbs, G. P., "Hybrid Active/Passive Control of Sound Radiation from Panels with Constrained Layer Damping and Model Predictive Control," *Proceedings of Noise-Con 2000*, Newport Beach, CA, Dec. 2000.

[4]Clarke, D., Mohtadi, C., and Tuffs, P., "Generalized Predictive Control - Part I. The Basic Algorithm," *Automatica*, Vol. 23, No. 2, 1987, pp. 137–148.

[5]Gibbs, G. P., Clark, R. L., Cox, D. E., and Vipperman, J. S., "Radiation modal expansion: Application to active structural acoustic control," *Journal of the Acoustical Society of America*, Vol. 107, No. 1, Jan. 2000, pp. 332–339.

[6]Plunkett, R. and Lee, C. T., "Length Optimization for Constrained Viscoelastic Layer Damping," *The Journal of the Acoustical Society of America*, Vol. 48, No. 1, 1970, pp. 150–161.

[7]Blevins, R. D., *Formulas for Natural Frequency and Mode Shape*, Krieger Publishing, Malabar, Florida, 1984.

[8]Elliott, S. J. and Johnson, M. E., "Radiation modes and the active control of sound power," *Journal of the Acoustical Society of America*, Vol. 94, No. 4, Oct. 1993, pp. 2194–2204.